Velocity Scaling of Shear Layer Noise induced by cold Jet flow with co-flowing Flight stream

Christian Jente*, Jan W. Delfs†

German Aerospace Center (DLR), Lilienthalplatz 7, D-38108 Braunschweig, Germany

Jet noise physics for normal velocity profiles are highly relevant operation states in the aerospace industry. Typically, a high velocity jet stream propagates into the surrounding sky and causes an airplane to move at a flight velocity which is smaller than the jet speed. The difference velocity between jet speed and flight speed has been identified to be a characteristic contributor for jet noise and historically has been in the focus for noise reduction. Even though jet noise could be fortunately reduced and is often not anymore the most prominent noise source, new interaction sources, such as jetf lap interaction noise, evoke the need for a fundamental understanding of its physics.

Lots of acoustic problems scale with a characteristic velocity which is proportional to a single flow potential. For example, cold jet noise scales according to Lighthill's famous $\mathbf{I \propto U_{jet}^8}$-analogy. With an additional co-flow, two flow potentials are present, namely flight speed and jet speed. The acoustically relevant velocity scaling speed depends on both of them, since the noise depends on the physical effects in the common shear layer.

This paper uses an ansatz from mixing layer theory which is used to approximate the acoustical source volume of the Lighthill equation for an isothermal shear layer. For low velocity ratios, the derivation results in the relation of $\mathbf{I \propto (\Delta U)^6 U_c^2}$, which claims that jet noise in co-flowing flight stream depends on power 6 of the velocity difference and the convection speed squared. The derivation allows for a hypothesis that for near unity velocity ratios, the relation changes into $\mathbf{I \propto (\Delta U)^4 U_c^4}$, whereby a transition into $\mathbf{I \propto (\Delta U)^5 U_c^3}$ at $\mathbf{r \approx 0.25}$ is suggested. Furthermore, the $\mathbf{I \propto (\Delta U)^6 U_c^2}$ scaling law is approximated wrt. formerly used ΔU scaling as $\mathbf{I \propto (\Delta U)^5 U_{jet}^3 \ldots (\Delta U)^4 U_{jet}^4}$, allowing for negligibly small error terms.

The velocity scaling is challenged by experimental data gathered at the Aeroacoustic Windtunnel in Braunschweig. Hereby, a variety of academic special cases, among others similar velocity profiles, similar shear layer mean velocities, similar difference velocities, as well as similar Strouhal numbers have been tested.

With the results from this paper, a new velocity scaling for jet noise has been proposed. If the scaling proves to be good against any jet noise data long term, the findings may help to improve the understanding about jet related noise challenges. The derived approximations for certain velocity profiles might also help characterize jet related problems, such as jet flap interaction noise or for investigating the role of inner shear layer mixing noise of dual stream engines with and without co-flowing flight stream.

*Research Engineer, Department of Technical Acoustics, christian.jente@dlr.de

†Head of Department, Technical Acoustics

Nomenclature

δ_ω	[m]	shear layer width
ΔU	[m/s]	difference velocity in shear layer
ΣU	[m/s]	$U_{jet} + U_\infty$, a measure for the shear layer propagation speed
ρ'	[kg/m³]	fluctuating density
ρ	[kg/m³]	density
ρ_∞	[kg/m³]	ambient density
$\boldsymbol{\tau}$	[kg/ms²]	shear stress tensor
τ	[s]	retarded time
θ	[°]	polar angle
a_∞	[m²]	speed of sound
A_{noz}	[m²]	nozzle outlet area of single stream nozzle
A_{st}	[m²]	source stretching factor[1]
A_{Byp}	[m²]	bypass nozzle outlet area
A_{Cor}	[m²]	core nozzle outlet area
c	[-]	convection parameter
c_{id}	[-]	convection parameter of an idealized trapezoid normal velocity profile
D	[m]	engine diameter at nozzle outlet (w/o nozzle TE)
D_{mix}	[m]	mixed (or equivalent) jet diameter
$\boldsymbol{e}_{r_0}$	[-]	unit vector
f	[Hz]	frequency
f_{nb}	[Hz]	narrowband frequency
H	[m]	vertical distance between engine MRP and flap MRP
$\boldsymbol{I}$	[-]	identity matrix
I	[W/m²]	Sound Intensity
L	[m]	horizontal distance between engine MRP and flap MRP
m	[-]	velocity scaling exponent for difference speed
n	[-]	velocity scaling exponent for convective speed
p'	[Pa]	fluctuating sound pressure
q	[-]	(overall) velocity scaling exponent
R	[m]	radial coordinate
r_U	[-]	velocity ratio
R_0	[m]	special radial position
$R_{1/2}$	[m]	jet half width
r_0	[m]	distance form source
SPL	[dB]	sound pressure level
SPL_{nb}	[dB]	narrowband sound pressure level
Sr	[-]	Strouhal number
T_{rr}	[-]	Lighthill's[2] turbulence stress tensor
U	[m/s]	streamwise velocity
U_∞	[m/s]	flight velocity
U_c	[m/s]	shear layer convection velocity
U_{jet}	[m/s]	jet velocity
$\overline{U}_s$	[m/s]	shear layer mean velocity
U_s	[m/s]	shear layer velocity
U'_s	[m/s]	shear layer velocity deviation
$\boldsymbol{v}$	[m/s]	velocity vector
V	[m³]	volume
x	[m]	streamwise engine coordinate
x_0	[m]	virtual origin of shear layer

AWB	Aeroacoustic Windtunnel Braunschweig
Def	definition
DLR	Deutsches Zentrum für Luft- und Raumfahrt e.V., i.e. the German Aerospace Center
ENG	centerpoint of engine (bypass) nozzle outlet, a measurement reference point
ISL	inner shear layer, between bypass flow and core flow
IVP	inverted velocity profile (outer velocity faster than inner velocity)
JFI	jet flap Interaction
mix	mixed jet property
nb	narrowband
NVP	normal velocity profile (inner velocity faster than outer velocity)
MRP	measurement reference point
OSL	outer shear layer, between ambient an bypass flow
p.	page
S/L	shear layer
TE	trailing edge
UHBR	ultra high bypass ratio
wrt	with respect to

I. Theory of Jet Acoustics with co-flowing flight stream

I.A. Problem Statement

The physical problem of jet acoustics with co-flowing flight stream consists of a circular jet which exits an engine nozzle and propagates with a characteristical jet speed U_{jet} into the ambient. The ambient is a constant co-flowing flight stream characterized by the flight speed U_∞. At the trailing edge of the nozzle exit, a shear layer (S/L) develops between jet and flight stream. The shear layer increases with increasing streamwise (x) position, whereas the jet's potential core decreases until it vanishes at $x/D_{mix} \approx 5$. At a distinct position x (in figure 1), a normal velocity profile (NVP) is portrayed, i.e. a velocity profile where the inner velocity is greater than the outer velocity. Characteristic velocities within the shear layer are the convection speed U_c, which is proportional to the propagation speed of the shear layer eddies, and the difference velocity $\Delta U = U_{jet} - U_\infty$, which is a measure proportional to the size of the shear layer eddies. The local shear layer width δ_ω is a limit for the maximum size of the local eddies. The virtual starting point of the shear layer is named x_0 and is merely introduced to account for realistic shear layer developments, where the virtual starting point may differ from the nozzle exit position, e.g. by a thick trailing edge or jet contraction due to real expansion. In the sketch (figure 1), an idealized shear layer $x_0 = 0$ is portrayed.

A characterizing parameter is the velocity ratio r_U, i.e. a dimensionless velocity, which is defined as

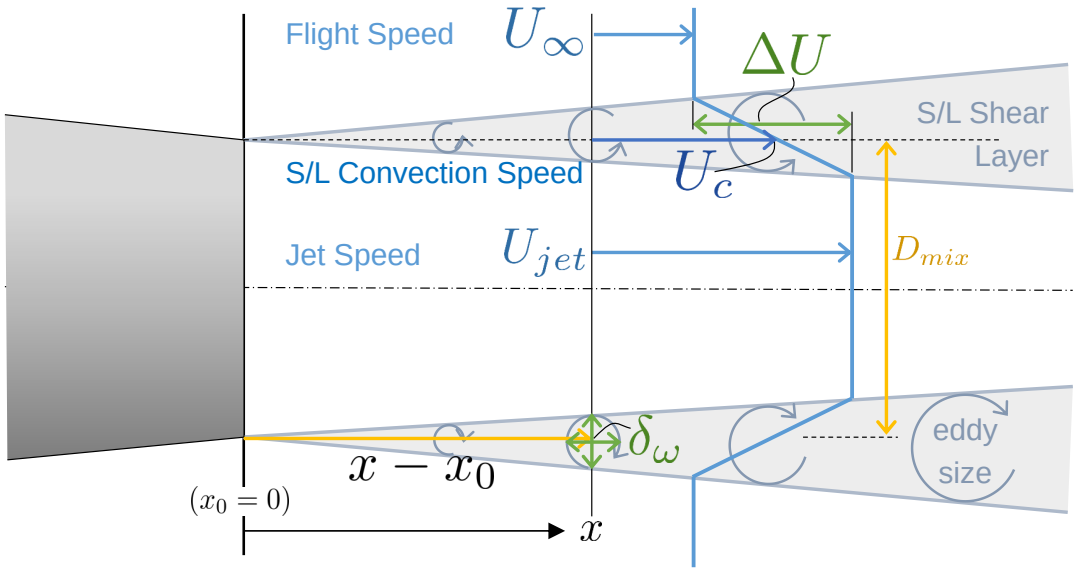

Figure 1: Shear Layer between flight and jet stream. Above symmetry line: relevant velocities, below symmetry line: characteristical geometries

the ratio of outer to inner speed. For jets in coflow, the velocity ratio r_U is defined as the ratio of flight velocity U_∞ to the jet speed U_{jet}. The comparison of velocity profiles with the same velocity ratio r_U simplifies the problem complexity, since two independent velocities (i.e. U_{jet} and U_∞) can be replaced by a single velocity component (e.g. U_{jet}) and a dimentionless parameter (i.e. r_U). Two velocity profiles shall be defined as similar to each other, if in terms of non-dimensionless velocity, they are identical, and in terms of absolute velocity they differ only by a scaling factor (compare figure 2).

I.B. Assumptions for estimation of Shear Layer Properties

One of the crucial characteristics of the physical problem is a good estimation of the shear layer convection speed U_c. In order to examine this, the velocity behind a single stream nozzle is measured by a rake of pressure probes. One velocity plot of the XZ-plane is displayed in figure 3). Drawing constant velocity isolines on the shear layer's outer part (closer to flight stream potential flow) results in lines which increase in radius with increasing streamwise direction. On the shear layer's inner part (closer to the jet potential core), there are isolines which decrease in radius with increasing streamwise position. In between, there is one velocity isoline which is located at a constant radius R_0 (mathematically expressed in equation 1 and portrayed in figure 3) for increasing streamwise position approximately within the entire initial mixing region of the jet. This velocity appears characteristic for the shear layer, since it is a constant along $0 \ldots 1 < x/D_{mix} < 5$ of the shear layer. Furthermore, the radial position where the

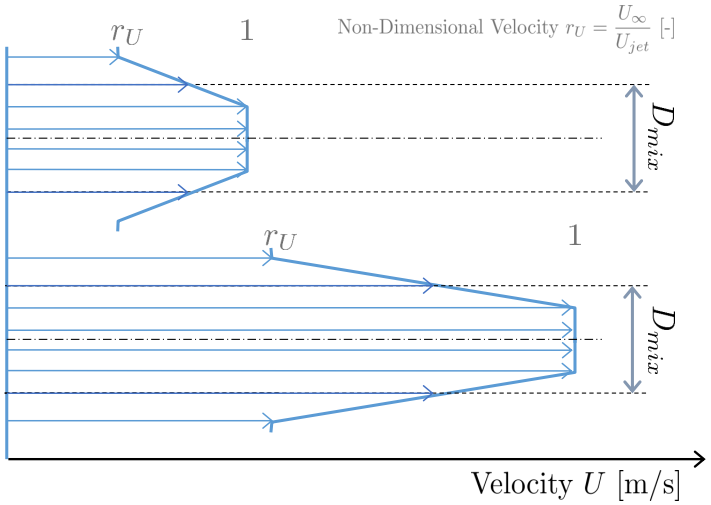

Figure 2: Two velocity profiles that fulfill the velocity similarity criterion $r_U = \text{const}$.

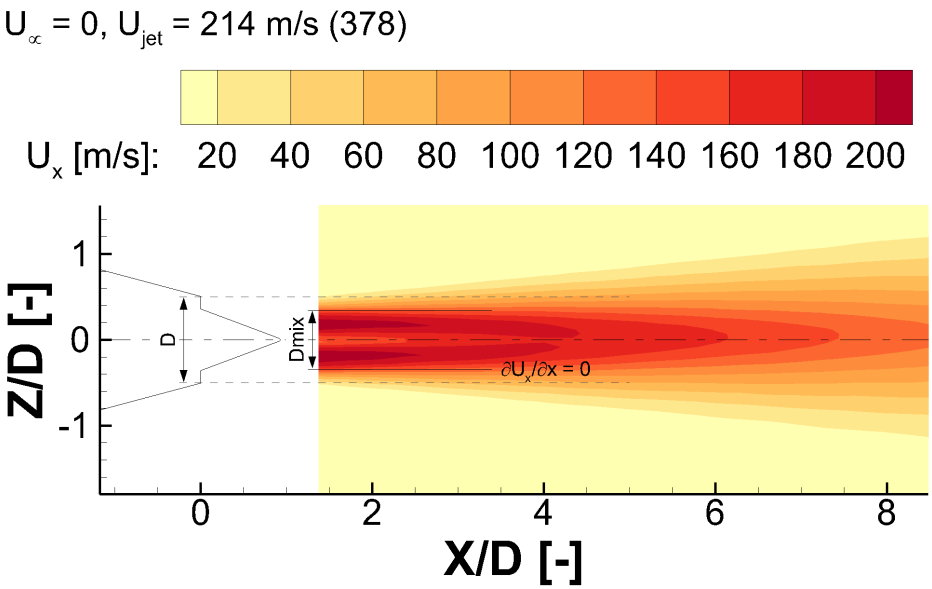

Figure 3: Flow downstream a coannular nozzle displayed in constant x-velocity isolines.

characteristic velocity can be observed, is independent of the nozzle exit velocity (compare figure 4).

$$\left.\frac{dU}{dx}\right|_{R_0=const} = 0 \tag{1}$$

By using experimental data, it can be shown that this constant radius R_0 fits very well to half of the mixing diameter D_{mix} of the nozzle (equation 2).

$$R_0 = D_{mix}/2 \tag{2}$$

For single stream nozzles, the mixing diameter is equivalent to the nozzle outlet diameter. For annular single stream flows, the mixing area is equivalent to the annular nozzle outlet area (when circularly redistributed in the free flow region) and therefore, the mixing diameter is smaller than the nozzle outlet diameter ($D_{mix} = 2 \cdot \sqrt{A_{noz}/\pi} < D$, compare figure 4, where the velocity isoline at the nozzle diameter D is not constant, but drifting away from the jet axis.). The mixing diameter for bypass nozzles depends on bypass ratio and its maximum is ($D_{mix} = 2 \cdot \sqrt{(A_{Byp} + A_{Core})/\pi} < D$):

$$D_{mix} = \begin{cases} D, & \text{single stream or long cowl dual stream nozzle} \\ 2 \cdot \sqrt{A_{noz}/pi}, & \text{annular nozzle} \\ \leq 2 \cdot \sqrt{(A_{Byp} + A_{Core})/\pi}, & \text{short cowl dual stream nozzle} \end{cases} \tag{3}$$

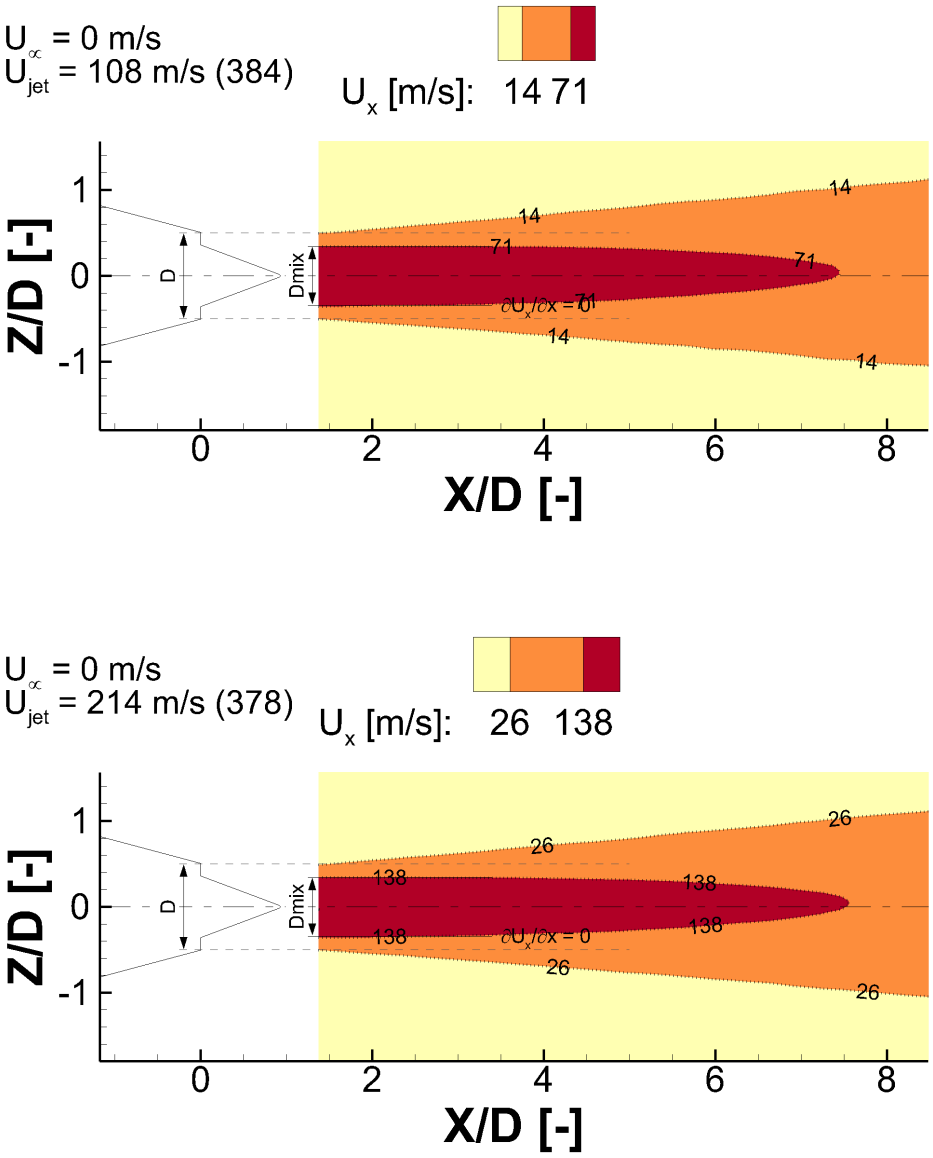

Figure 4: Localization of a characteristical shear layer speed at jet mixing diameter.

An interesting challenge concerns the value of the convective speed, defined like (equation 4).

$$U_c := U(R_0) = U(D_{mix}/2) \tag{4}$$

The convective speed shall be described as the product of the sum of jet and flight velocity with a convection parameter c, which is assumed to be mainly dependent on the velocity ratio r_U, but also on the shape function of the velocity profile.

$$U_c = c(r_U) \cdot \Sigma U \tag{5}$$

$$\Sigma U = U_{jet} + U_\infty \tag{6}$$

For dimensional approximations, the mean is often taken to approximate convection speed, i.e. $c(r_U) = 1/2$ (equation 5). In mixing layer theory, the half width $R_{1/2}(x)$ of a jet is introduced, which is the local position of the mean shear layer velocity $(U_{jet} + U_\infty)/2$. However, the proposed criterion (equation 1) cannot be met for $c(r_U) = 1/2$, and for normal velocity profiles, the mean velocity isoline drifts away from the engine axis with increasing streamwise direction. This can be observed in figure 4, where the identified velocity of $U_c \approx 71\,\mathrm{m/s}$ is significantly higher than the shear layer mean velocity $\bar{U} = 0.5 \cdot 108\,\mathrm{m/s} = 54\,\mathrm{m/s}$. This means, that for normal velocity profiles, the convective speed of the shear layer is greater than the mean.

Different authors suggested other convective speeds, e.g. Fuchs and Michel[3] found $c(r_U = 0) = 0.65$ for jets without coflow.

I.C. A simplified mean pressure function c_{mp}

The mixing speed of the inner shear layer of dual stream flows is calculated by using the momentum equation, an equation that balances forces. However, the use of extensive flow properties is necessary, i.e. the bypass and core mass flow rates. This is possible because of their character as two internal flows. For the outer shear layer, a mass flow rate based analogy cannot be used, since the ambient is characterized by an ideally infinite volume. The external flow cannot be characterized by extensive flow properties. Therefore, another mechanism must be found to identify the velocity at the boundary between jet and ambient. A first approach is to use a force-based postulation where it is assumed that at the mixed diameter position, the shear layer centroid is located. If this is true, then the centroid velocity can be calculated by calculating the mean of the dynamic pressures. (Since the static pressure is assumed to be constant (subsonic) outlet condition, the mean of the total pressure can also be chosen to calculate the centroid velocity.)

$$\overline{\Delta p} = 1/2 \cdot (\Delta p_{jet} + \Delta p_{\infty}) \tag{7}$$

In order to get a simple relation for the convection parameter, the assumption of constant density is made. Note, that with the subsonic outlet condition $p = const$ and a unity total temperature profile (where $T_{0,\infty} = T_{0,jet}$), static temperatures (and thus density) for very large subsonic Mach numbers $M = 1$ are off by factor 1.2 compared to $M = 0$.

$$\frac{T_0}{T} = \left(1 + \frac{\gamma - 1}{2} \underbrace{M}_{=1}^{\,2}\right) = 1.2 \tag{8}$$

Using the formula for dynamic pressure, $\Delta p = \rho/2 \cdot U^2$, and the velocity ratio, the centroid value can be calculated.

$$U_{c,mp}^2 = 1/2 \cdot (U_{jet}^2 + U_{\infty}^2) \tag{9}$$

$$U_{c,mp} = U_{\infty} \frac{\sqrt{2}}{2} \sqrt{1 + \frac{1}{r_U^2}} \tag{10}$$

$$c_{mp} = \frac{U_{c,mp}}{U_{jet} + U_{\infty}} = \frac{r_U}{1 + r_U} \left(\frac{\sqrt{2}}{2} \sqrt{1 + \frac{1}{r_U^2}}\right) \tag{11}$$

$$c_{mp} = \frac{\sqrt{2}}{2} \frac{\sqrt{1 + r_U^2}}{1 + r_U} \tag{12}$$

This model shows the right trend, but unfortunately does not correlate well with the measured data (see 6).

I.D. The idealized trapezoid approximation c_{id}

A better approximation is to use a fit function between the two known boundary values: For an ideal unity velocity profile ($r_U = 1$), the shear layer convection velocity is $U_c = 1/2 \cdot \Sigma U$, i.e. $c(r_U = 1) = 1/2$, and for an idealized triangular shear layer profile ($r_U \to 0$) , the velocity at the centroid is $U_c \approx 2/3 \cdot \Sigma U$, i.e. $c(r_U \to 0) = 2/3$, which fits well with Fuchs' and Michel's experimental value of $c(r = 0) = 0.65$. One could argue that physically relevant velocity profiles should be defined as continuously differentiable which would "round out" the break points and thus, decrease the centroid velocity below $U_c = 2/3 \cdot \Sigma U$. However, this is only possible if the "round out" between shear layer and jet is counted to the jet (as in figure 5). With these assumptions, $c(r_U) \approx 2/3$ could be an upper boundary for normal velocity profiles.

$$\underbrace{1/2}_{r \to 1} \leq c(r_U) < \underbrace{2/3}_{r=0} \tag{13}$$

Even though this function describes the centroid velocity of an idealized trapezoid-like normal velocity profile, it should be rather counted as a fitting function or approximation, since velocity by itself is not known as a conservation property.

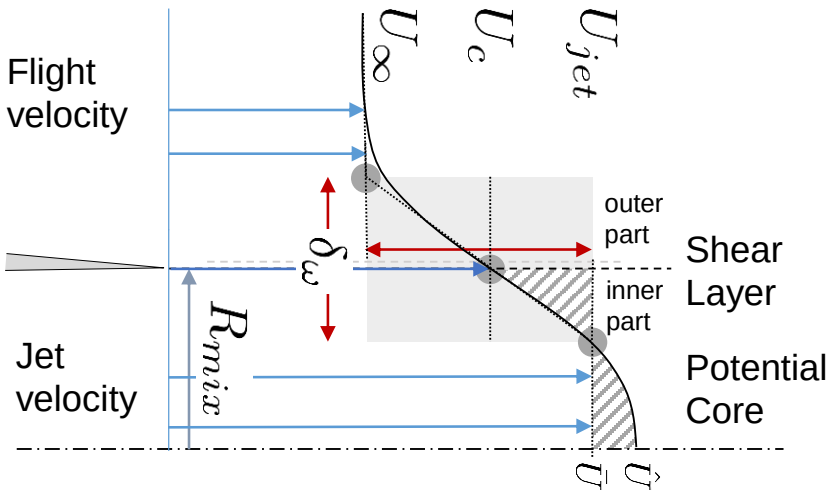

Figure 5: Steady (black) and discretized (blue) velocity profile model, where the jet velocity is the mean velocity $U_{jet} = \bar{U}$ within the boundaries of the mixed jet radius R_{mix} and thus the shear layer is similar to a trapezoid.

The derivation uses the centroid formula for combined single centroids for rectangle and triangle (equation 14).

$$R_c = \frac{\Sigma_i R_{c,i} A_i}{\Sigma_i A_i} \tag{14}$$

Note, how A_i is the integrated "area" underneath the velocity profile curve of dimension velocity times length (equation 15.

$$R_c = \frac{\left(\frac{2}{3}\delta_\omega\right)\frac{\delta_\omega \cdot \Delta U}{2} + \left(\frac{1}{2}\delta_\omega\right)\delta_\omega U_\infty}{\frac{1}{2}\delta_\omega \cdot \Delta U + \delta_\omega U_\infty} \tag{15}$$

$$\frac{R_c}{\delta_\omega} = \frac{2}{3} \cdot \frac{U_{jet} - U_\infty}{U_{jet} + U_\infty} + \frac{U_{jet}}{U_{jet} + U_\infty} \tag{16}$$

The idealized convection parameter reduces to the triangular centroid (for $r = 0$) and rectangular centroid (for $r = 1$, see equation 17.

$$c_{id}(r_U) := \frac{R_c}{\delta_\omega} = \frac{2}{3} \cdot \frac{1 - r_U}{1 + r_U} + \frac{r_U}{1 + r_U} \tag{17}$$

The convection parameter of idealized NVPs is plotted in figure 6 where it is also compared against a small set of experimental velocity profiles. As expected, the values of real rounded velocity profiles without any breakpoints fulfills the criterion of slightly smaller centroid values $c < c_{id}$.

I.E. Sensitivity of sound intensity w.r.t. velocity ratio r_U

Note, that the different values of the function c have implications on velocity scaling with the mean speed $\overline{U} \propto \Sigma U$ instead of convection velocity U_c. Take the example of two velocity profiles with the same shear layer mean velocity, but a different set of jet and flight speed. Let us assume a dependency of sound intensity scaling with convection velocity squared.

$$I \propto U_c^2 = c(r_U)^2 \Sigma U^2 \tag{18}$$

$$SPL \propto 20\,\mathrm{lg}\left(c(r_U)\right) + 20\,\mathrm{lg}\left(\Sigma U\right) \tag{19}$$

The maximum velocity scaling error between both of the profiles is $\Delta SPL \approx 2.50\,\mathrm{dB}$ (equation 21).

$$[\Delta SPL]_{r\to 1}^{r\to 0} = 20\,\mathrm{lg}\left(\frac{2/3}{1/2}\right) + 20\,\mathrm{lg}\left(\frac{\Sigma U}{\Sigma U}\right)^{\to 0} \tag{20}$$

$$[\Delta SPL]_{r\to 1}^{r\to 0} = 20\,\mathrm{lg}\left(\frac{4}{3}\right) \approx 2.50\,\mathrm{dB} \tag{21}$$

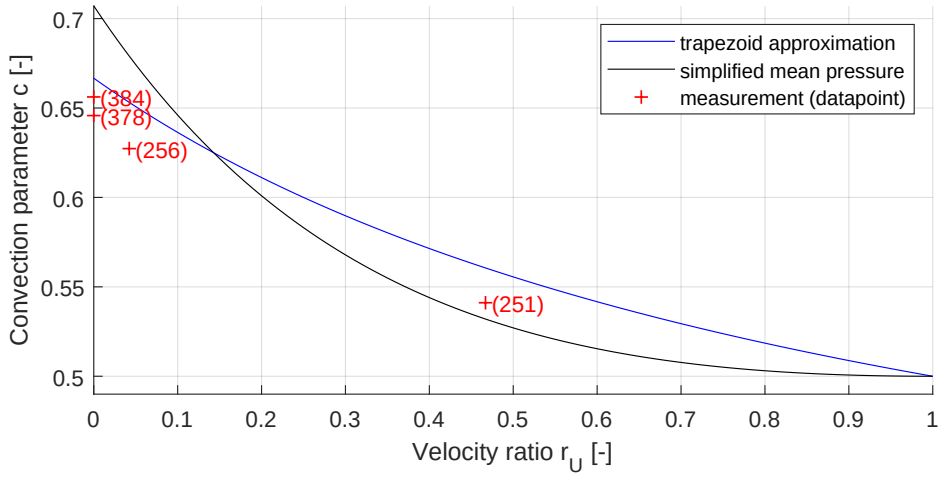

Figure 6: Approximation for the convection parameter and experimental data (data plots are partly displayed in figures 4)

For another assumed dependency of sound intensity scaling directly with the convection velocity, the velocity scaling error due to function c is $\Delta SPL \approx 1.25\,\mathrm{dB}$. Note, however, that for a variety of velocity profiles with rather similar velocity ratio r_U, this type of scaling error can be neglected.

I.F. Ansatz

The new idea to solve the Lighthill equation[2] is based on the estimation of the source volume which accounts for the acoustically relevant source volume by using a similarity from the shear layer theory (see Eisfeld[4]). For this paper, a similarity from the mixing layer theory of turbulent flows is used (equation 22), which sets the turbulent shear layer width δ_ω at the local position x in relationship to the the difference shear layer velocity ΔU and shear layer convection velocity U_c.

$$\frac{\delta_\omega(x)}{x - x_0} \propto \frac{\Delta U}{U_c} \tag{22}$$

Note, how this relationship (compare figure 1) can be derived by applying an intercept theorem type of approach. Also note, that the mixing layer theory approach uses the shear layer mean velocity $\bar{U}$, which equals the convection velocity at the velocity ratio of $r_U = 1$.

$$U_c = \begin{cases} \frac{1}{2} \cdot \Sigma U, & \text{mixing layer theory, } r_U \to 1 \\ c(r_U) \cdot \Sigma U, & \text{used in this paper, } 0 < r_U \ll 1 \end{cases} \tag{23}$$

The reformulation of equation 22 is a measure for the retarded time (24).

$$\Delta\tau \propto \frac{\delta_\omega(x)}{\Delta U} \propto \frac{x - x_0}{U_c} \tag{24}$$

I.G. Normalization of frequency

With several prospective characteristic velocities and geometries available, different definitions for the Strouhal number may be suggested. The first canditate which comes into mind, is a commonly used equation referenced to the difference velocity and mixed jet diameter D_{mix}.

$$Sr_{D_{mix}} \propto \frac{f \cdot D_{mix}}{\Delta U} \tag{25}$$

This definition suggests that the Strouhal number is similar for the same nozzle as long as the difference velocity between jet velocity and flight velocity remains identical. Note, that the comparison of narrow-band testdata for two datapoints indicates that the frequencies appear to be rather fixed. Therefore, the Strouhal numbers of those two datapoints should be already "fairly similar". In praxis, this is not the case.

As a second candidate, let us examine a definition which is to some extent analogously defined as in van Kármán's vortex street. The characteristical geometry is the local eddy size (proportional to the shear layer width δ_ω). Such an eddy propagates with the shear layer convection speed U_c (equation 26):

$$Sr_{\delta_\omega} = \frac{f \cdot \delta_\omega}{U_c} \tag{26}$$

Here, the shear layer width δ_ω can be replaced using equation 22:

$$Sr_x \propto \frac{f}{c(r_U) \cdot \Sigma U} \cdot \frac{\Delta x \cdot \Delta U}{c(r_U)\Sigma U} \tag{27}$$

Since the eddies grow in streamwise direction x, a distinct location Δx could be defined, e.g. at the end of the jet potential core, where $\Delta x \approx 5 \cdot D_{mix}$. In other words, location Δx and mixing diameter D_{mix} formulate a characteristical proportionality or aspect ratio of the physical problem.

$$Sr_{x \propto D_{mix}} \propto \frac{f}{c(r_U) \cdot \Sigma U} \cdot \frac{D_{mix} \cdot \Delta U}{c(r_U)\Sigma U} \tag{28}$$

$$\tag{29}$$

Using the velocity ratio, the Strouhal number definition can be redefined wrt. to a characteristic velocity of choice and error terms to formerly used definitions calculated.

$$Sr \propto \frac{f \cdot D_{mix}}{\Delta U} \cdot \frac{(1 - r_U)^2}{c^2 \cdot (1 + r_U)^2} \tag{30}$$

$$Sr \propto \frac{f \cdot D_{mix}}{U_{jet}} \cdot \frac{(1 - r_U)}{c^2 \cdot (1 + r_U)^2} \tag{31}$$

$$Sr \propto \frac{f \cdot D_{mix}}{U_c^2} \cdot \frac{(1 - r_U)}{(1 + r_U)} \tag{32}$$

I.H. Derivation of the Normalization wrt. velocity

In order to derive the velocity scaling law, Lighthill's[2] turbulence stress tensor T_{rr} (1) as well as the source volume dV (2) need to be estimated (equation 33):

$$p'(\boldsymbol{x}, t) = \frac{1}{4\pi r_0 a_\infty^2} \int_{V_\infty} \underbrace{\ddot{T}_{rr}}_{(1)} \underbrace{dV}_{(2)} \tag{33}$$

1. Lighthill's turbulence stress tensor T_{rr} is simplified for cold jet flow (equation 34): Changes of velocity (term 1) are relevant, changes of entropy (term 2) are neglected for isothermal jet flow and changes in the viscous friction stresses are dimensionally negligible.

$$T_{rr} := \boldsymbol{e}_{r_0} \cdot \big([\rho \boldsymbol{v}\boldsymbol{v} + \cancelto{0}{(p' - a_\infty^2 \rho')} \boldsymbol{I} - \cancel{\boldsymbol{\tau}}] \cancelto{0}{\boldsymbol{e}_{r_0}} \big) \tag{34}$$

$$\tag{35}$$

The first time derivative of $\rho \boldsymbol{v}\boldsymbol{v}$ uses the product rule (equation 36) and evaluated for 1D shear layer flow with Reynolds decomposed shear layer velocity $U_s = \overline{U}_s + U'_s$. The second time derivative uses this result and produces two terms (equation 37) which need to be dimensionally compared against each other. In the further derivation, it is assumed that the product of first order time derivates is greater than the second order time derivated term.

$$\frac{\partial \boldsymbol{T}}{\partial \tau} \propto \rho_\infty \Big[\frac{\partial \boldsymbol{v}}{\partial \tau} \boldsymbol{v} + \boldsymbol{v} \frac{\partial \boldsymbol{v}}{\partial \tau} \Big] \propto \rho_\infty \frac{\partial U'_s}{\partial \tau} U_s \tag{36}$$

$$\frac{\partial^2 \boldsymbol{T}}{\partial \tau^2} \propto \rho_\infty \Big[\underbrace{\frac{\partial^2 U'_s}{\partial \tau^2} U_s}_{A} + \underbrace{\frac{\partial U'_s}{\partial \tau} \frac{\partial U'_s}{\partial \tau}}_{B} \Big] \tag{37}$$

The shear layer mean velocity is proportional to the sum of jet and flight velocity (equation 38), whereas the shear layer fluctuation velocity is proportional to the difference of both velocities

(equation 39). With the approximated time derivative in equation 40, the time derivations to the Lighthill turbulence stress tensor can be approximated (equation 41).

$$\overline{U}_s \propto (U_{jet}+U_\infty) \tag{38}$$
$$U'_s \propto (U_{jet}-U_\infty) \tag{39}$$
$$\frac{\partial}{\partial\tau} \propto \frac{1}{\Delta\tau} \propto \frac{U'_s}{\delta_\omega} \tag{40}$$
$$\frac{\partial^2 \boldsymbol{T}}{\partial\tau^2} \propto \frac{\rho_\infty}{\delta_\omega^2}(U'_s)^4 \tag{41}$$

Note, that if term A and term B in equation 37 were in fact dimensionally similar, the dimensional estimation would depend on weighing the importance of the shear layer mean velocity $\overline{U}_s$ against the shear layer difference velocity ΔU (see equation 42 and 43). The criterion of $r = 1/3$ sets apart velocity profiles with greater difference velocity for $r < 1/3$ and velocity profiles with greater shear layer mean velocity ($r > 1/3$).

$$\Delta U = \overline{U}_s \tag{42}$$
$$U_{jet} - U_\infty = \frac{1}{2}(U_{jet} + U_\infty) \tag{43}$$
$$U_\infty = \frac{1}{3}U_{jet} \tag{44}$$

(Note, that a comparison of the shear layer difference velocity against the convection speed (equation 45) for an idealized trapezoid NVP (using equation 17) would reduce the critical velocity ratio to $r = 1/4$ (equation 47). Thus, for real velocity profiles, the transition between shear layer vs. propagation dominating flow might be expected somewhere in between $r > 1/4 \ldots 1/3$, which makes $r = 1/3$ an upper limit.)

$$\Delta U = U_c \tag{45}$$
$$U_{jet} - U_\infty = \underbrace{c_{id}}_{1/2\ldots2/3}\ (U_{jet} + U_\infty) \tag{46}$$
$$U_\infty = \frac{1}{4}U_{jet} \tag{47}$$

Lighthill's turbulence stress tensor might then be estimated as in equation 49 for $r \gg 1/3$ which would therefore result in an $I \propto\!\!\!\sim \Delta U^4 (\overline{U}_s)^4$ velocity scaling law.

The changing velocity scaling law hypothesis In other words, if in general none of the terms A and B (in equation 37) can be estimated dimensional larger and they are of similar dimensions, , then there is a chance for a change velocity scaling law depending on the velocity ratio of the profile. This would result in the following results:

$$I \propto \begin{cases} (\Delta U)^6 \cdot U_c^2, & B \gg A, \text{ for strong NVP, } r_U \to 0 \\ \approx (\Delta U)^5 \cdot U_c^3, & A \approx B, \text{ for intermediate NVP, } r_U \approx 0.25 \ldots 0.33 \\ (\Delta U)^4 \cdot U_c^4, & A \gg B, \text{ for unity VP, } r_U \to 1 \end{cases} \tag{48}$$

However, the measurement data used in this paper is not suited for a thorough test of such a hypothesis. Therefore, this paper continues with the derivation of the terms which possibly suits the measurement data best ($B \gg A$):

$$\frac{\partial^2 \boldsymbol{T}}{\partial\tau^2} \propto \frac{\rho_\infty}{\delta_\omega^2}(U'_s)^3 \cdot \overline{U}_s \tag{49}$$

2. Acoustic Source Volume. For slim shear layers $\delta_\omega \ll D_{mix}$ the source volume can be estimated without using the exact inner and outer radius (equation 50). The shear layer width δ_ω between

jet and flight stream can be approximated with the 1D mixing layer theory ansatz (equation 51).

$$dV \propto \delta_\omega \pi D_{mix} dx \tag{50}$$

$$\delta_\omega \propto \frac{\Delta U}{U_c} \cdot (x - x_0) \tag{51}$$

$$dV \propto \pi D_{mix} \frac{\Delta U}{U_c} \cdot (x - x_0)\, dx \tag{52}$$

$$\Delta V \propto \pi D_{mix} \frac{\Delta U}{U_c} \cdot \tfrac{1}{2} (x - x_0)^2 \tag{53}$$

$$\Delta V \propto \pi D_{mix} \frac{U_c}{\Delta U} \cdot \tfrac{1}{2} \delta_\omega^2 \tag{54}$$

The results for the approximation of Lighthill's turbulence stress Tensor (equation 41) and the source volume (equation 54) are inserted into the starting equation (equation 33). The resulting pressure fluctuation (equation 55) can be used to estimate sound intensity I (equation 56).

$$p' \propto \frac{\alpha^2 \rho_\infty}{r_0 a_\infty^2} (\Delta U)^3 (U_c) \cdot D_{mix} \tag{55}$$

$$I = \overline{p' \boldsymbol{v}'} \propto \frac{\overline{p'^2}}{\rho_\infty a_\infty} \tag{56}$$

$$I \propto \frac{\rho_\infty D_{mix}^2}{r_0^2 a_\infty^5} \, (U_{jet} - U_\infty)^6 \, (U_c)^2 \tag{57}$$

I.I. Velocity Scaling wrt. different velocity related variables

The derivation can be reformulated with respect to different velocity related variables:

$$I \propto \frac{\rho_\infty D_{mix}^2}{r_0^2 a_\infty^5} \, (U_{jet} - U_\infty)^6 \cdot c(r_U)^2 \, (U_{jet} + U_\infty)^2 \tag{58}$$

$$I \propto \frac{\rho_\infty D_{mix}^2}{r_0^2 a_\infty^5} \, (\Delta U)^6 \cdot c(r_U)^2 \, (\Sigma U)^2 \tag{59}$$

$$I \propto \frac{\rho_\infty D_{mix}^2}{r_0^2 a_\infty^5} \, U_{jet}^8 \left(1 - \frac{U_\infty}{U_{jet}}\right)^6 \cdot c(r_U)^2 \left(1 + \frac{U_\infty}{U_{jet}}\right)^2 \tag{60}$$

$$I \propto \frac{\rho_\infty D_{mix}^2}{r_0^2 a_\infty^5} \, U_{jet}^8 \, (1 - r_U)^6 \cdot c(r_U)^2 \, (1 + r_U)^2 \tag{61}$$

In the past, a few attempts have been made to account for source volume stretching. The interested reader may refer to Michalke and Michel,[1] who introduced a jet stretching factor A_{st}. Their derivation for an isothermal jet at a polar angle of $\theta = 90\,^\circ$ looks very similar to equation 61 for $q = 8$ and $A_{st} = 2$:

$$I \propto U_{jet}^q \, (1 - r_U)^{q-2} \cdot \left[1 + (A_{st} - 1) r_U\right]^2 \tag{62}$$

Michalke and Michel made the following observations (Appendix 2 of their paper[1]):

- $A_{st} = 1$ for a particle moving along the jet axis with in the potential core
- $A_{st} > 1$ for path lengths greater than the length of the potential core
  - $A_{st} \approx 2$ for a particle moving in the middle of the mixing region
  - $A_{st} = 1.5 \ldots 3$ relevant for low frequency region which contains the peak of the spectrum
  - even greater A_{st} for more rapidly decaying axial velocity profiles, e.g. for a mixer nozzle

This suggests that the high frequency part of the spectra collapse at $q = 6$ (where the low frequency part of the spectrum still underscales) and the low frequency parts collapse approximately at $q = 8$ (where the high frequency part of the spectrum should slightly overscale). When testing those findings against data (see figure 7), there is good agreement to this statement.

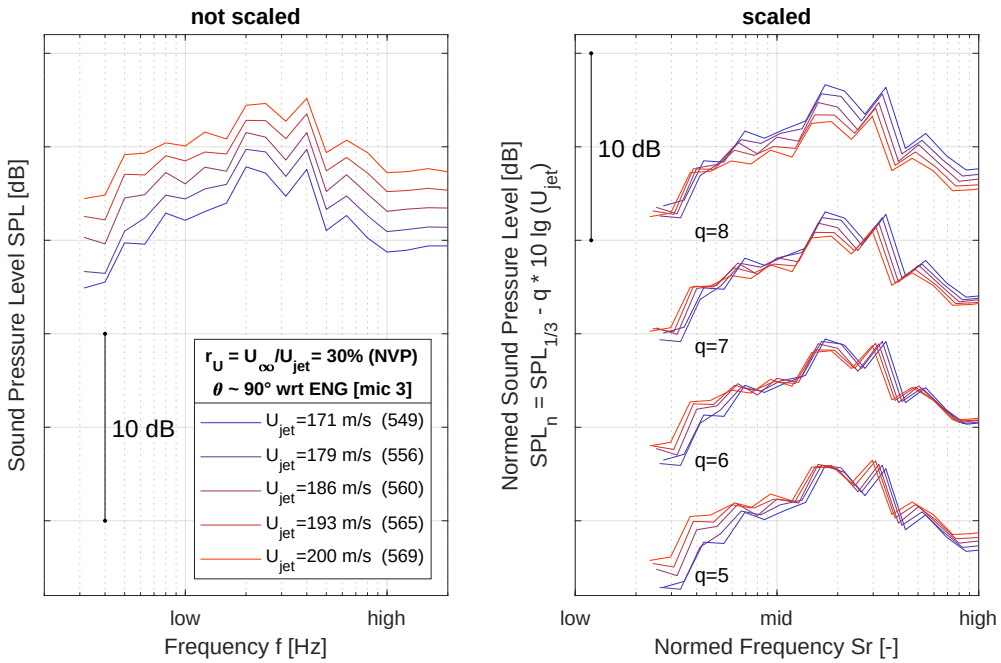

Figure 7: $I \propto U_{jet}^{q}$ velocity scaling for $r_U = 30\,\%$=const. Note, that the high frequencies collapse well for $q = 6$ and low frequencies for $q = 8$.

II. Acoustic Measurements and Analysis

II.A. Test Setup

The test was conducted in the Aeroacoustic Windtunnel Brauschweig (AWB), a DLR testing facility in Northern Germany. An isolated nozzle was installed to the pressureized air supply, where jet velocities are limited to the maximum volumetric flow rate of $Q = 9100\,\mathrm{Nm^3/h}$ and flight velocities to a maximum of approximately $U_\infty = 60\,\mathrm{m/s}$. Background noise has been measured for flight stream alone (i.e. without jet flow).

Acoustic data is recorded by a microphone setup which is placed in a straight line underneath the nozzle ($\psi = 180\,^\circ$) spanning polar angles of ($\theta = 66\,^\circ \ldots \theta = 135\,^\circ$).
The noise spectra have been corrected with respect to microphone free field characteristics and microphone directivity, shear layer refraction (incl. wave convection), atmospheric absorption (Sutherland), as well has convective amplification. The propagation radius is normalized to $r = 1\,\mathrm{m}$.

II.B. Analysis with narrowband scaled data

The velocity scaling for the narrowband is applied similarly to the derivation of Gaeta and Ahuja[5] for isolated jet noise data. For the changed physical setting from a non co-flow to a co-flow problem, the characteristic velocity and length scale of the Strouhal number definition in equation 30 has been used. Note, that a polar angle of $\theta = 90\,^\circ$ has been chosen, in order to neglect the Doppler frequency correction factor for simplicity reasons.

$$Sr_{norm} = f_{nb} \cdot \frac{D_{jet} \cdot \Delta U}{c^2 \left(\Sigma U\right)^2} \tag{63}$$

$$SPL_{norm} = \underbrace{SPL_{nb} - 10 \cdot \lg\left(\Delta f\right)}_{PSD} - 10 \cdot \lg\left(\frac{D_{mix}}{\Delta U} \cdot \frac{(1 - r_U)^2}{c^2 \cdot (1 + r_U)^2}\right) \tag{64}$$

III. Experimental Velocity Scaling results

The experimental approach for finding the velocity scaling is a decomposition of the scaling exponents. With the previous derivations (equation 57), it is assumed that the sound intensity scales with difference velocity and convection speed (equation 65). For finding velocity scaling results experimentally, the exponents m and n are assigned. For jet flow without co-flow (equation 66), the velocity scaling law depends on the jet scaling coefficient, here assigned as q, which is presumedly the sum of m and n (equation 67).

$$I \propto \Delta U^m \cdot {U_c}^n \tag{65}$$

$$\lim_{U_\infty \to 0} I \propto U_{jet}^q \tag{66}$$

$$q = m + n \tag{67}$$

III.A. The dependency on power 8 jet speed

If the derivation of the velocity scaling law is correct, then self-similar velocity profiles (r_U =const) scale with $I \propto U_{jet}^8$ (see equation 68). In order to test this hypothesis, test data of strong NVP has been scaled by velocity. The velocity ratios are $r_U = 0.2$ (figure 8), $r_U = 0.25$ (figure 9) and $r_U = 0.30$ (figure 10), where the difference velocities of the scaled jets differ between $\Delta U = 120\,\mathrm{m/s}$ and $\Delta U = 140\,\mathrm{m/s}$. Note, that the normalization of the frequency (including the special case of the isolated jet $r_U = 0$) can be done by scaling wrt. any characteristic velocity, as the velocity profiles are similarly scalable (compare equations 30 to 32).

$$I \propto U_{jet}^8 \cdot \cancel{(1 - r_U)^6 (1 + r_U)^2} \underbrace{(c(r_U))^2}_{\approx \mathrm{const}} \quad \cancel{\rightarrow} \; r_U = \mathrm{const} \tag{68}$$

Experiments with similar velocity profiles can be a means to find out whether the test facility allows for U_{jet}^8-scaling or whether other noise sources, e.g. test rig noise are significant. The unscaled data shows a significant SPL difference of approximately $\Delta SPL = 6\,\mathrm{dB}$. The scaled spectra show:

- for $q = 6$ an underscaling of the low frequency peak and matching high frequency parts (those are also the findings of Michalke and Michel[1]),
- slight to no underscaling of the low frequency peak for $q = 7$, as well as
- slight overscaling for $q = 8$ (especially for $r_U = 0.2$).

The theoretical expectation for the velocity scaling with self-similar velocity profiles should result in a clear indication for low-frequency peak scaling at $q = 8$. However, the experimental results show slight overscaling for $q = 8$ and may rather suggest $q = 7 \ldots 8$. Michalke's and Michel's derivation would solve this by slightly adjusting the stretching factor A_{st}.

The neglected convection parameter c, which depends on velocity ratio r_U and shape function of the velocity profile, is approximately constant and might rather not be an explanation for overscaling. However, slight overscaling of lower jet velocities might be even typical, as other authors, i.a. Gaeta and Ahuja[5] as well as Michel and Michalke[1] stated the same effect.

Note, that if $q = 8$ (e.g. for a hot jet) cannot be solemnly established, then in the following analysis, one or both of the exponents m and n may not respond to the theoretical derivations.

III.B. The dependency of the convection speed

Velocity profiles with constant difference speed $\Delta U = U_{jet} - U_\infty$ scale with $I \propto U_c^2$ for low velocity ratios according to the derivation in equation 57. If the velocity ratios are in close vicinity, yet produce distinguishable velocity profiles, the convection parameter $c(r_U)$ may be neglected for the normalization of the frequency. Note, that the narrowband velocity scaling can be conducted using the mean velocity $\overline{U}$ or velocity sum ΣU (since $2\overline{U} = \Sigma U$) as characteristic scaling velocity (see equation 69).

$$I \propto (c(r_U))^2 (\Sigma U)^2 \cdot \cancel{(\Delta U)^6} \quad \cancel{\rightarrow} \; const. \tag{69}$$

$$Sr \propto \frac{f \cdot D_{mix}}{(c(r_U))^2 \cdot (\Sigma U)^2} \cdot \cancel{\Delta U} \quad \cancel{\rightarrow} \; const. \tag{70}$$

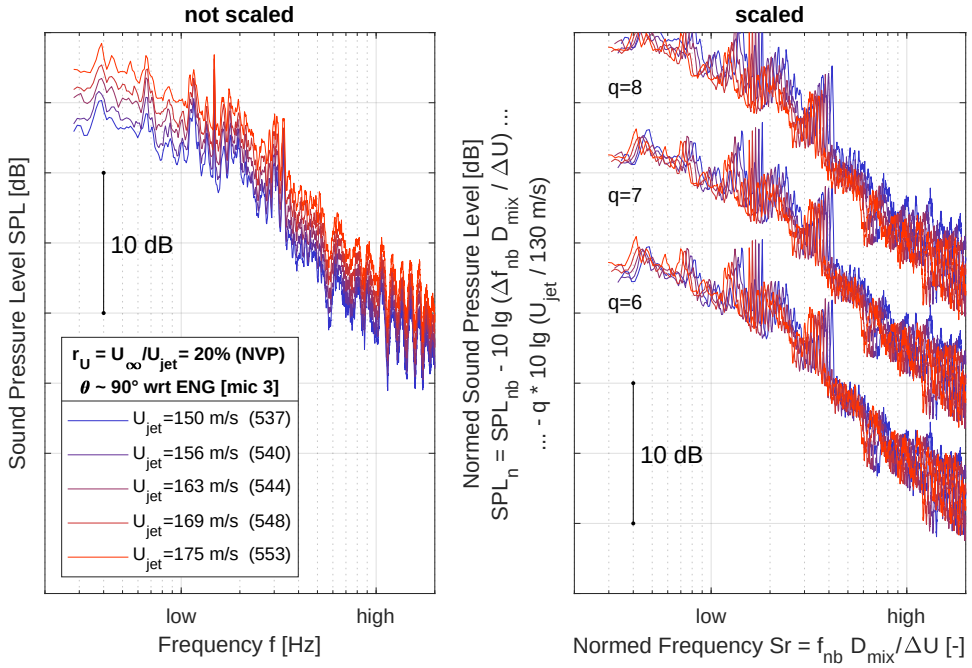

Figure 8: $I \propto U_{jet}^{q}$ velocity scaling for $r_U = 20\,\%$=const.

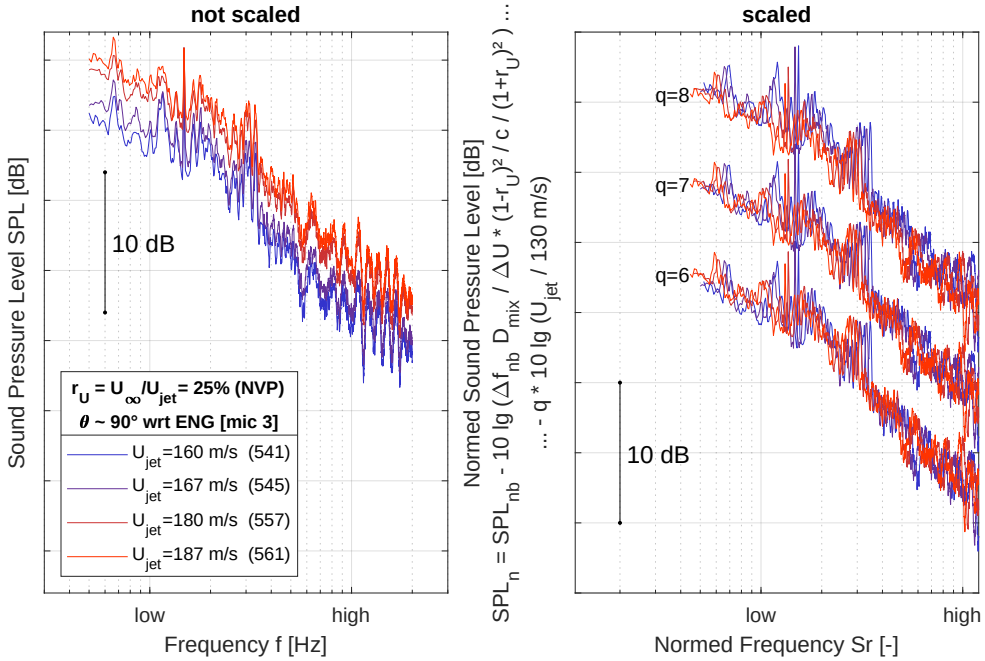

Figure 9: $I \propto U_{jet}^{q}$ velocity scaling for $r_U = 25\,\%$=const.

In order to challenge the assumed power 2 convection velocity scaling, constant difference velocities of $\Delta U = 120\,\mathrm{m/s}$ (figure 11), $\Delta U = 125\,\mathrm{m/s}$ (figure 12), $\Delta U = 135\,\mathrm{m/s}$ (figure 13) and $\Delta U = 140\,\mathrm{m/s}$ (figure 14) have been defined. Normal velocity profiles with velocity ratios of $r_U = 0.2$ to $r_U = 0.3$ produce spectra with an (unscaled) sound pressure level difference of $\Delta SPL \leq 5\,\mathrm{dB}$. This SPL peak difference is significant, since it confirms the theory that the velocity scaling is not only dependent on the difference velocity, but needs another velocity scaling component (e.g. the one derived in this paper).

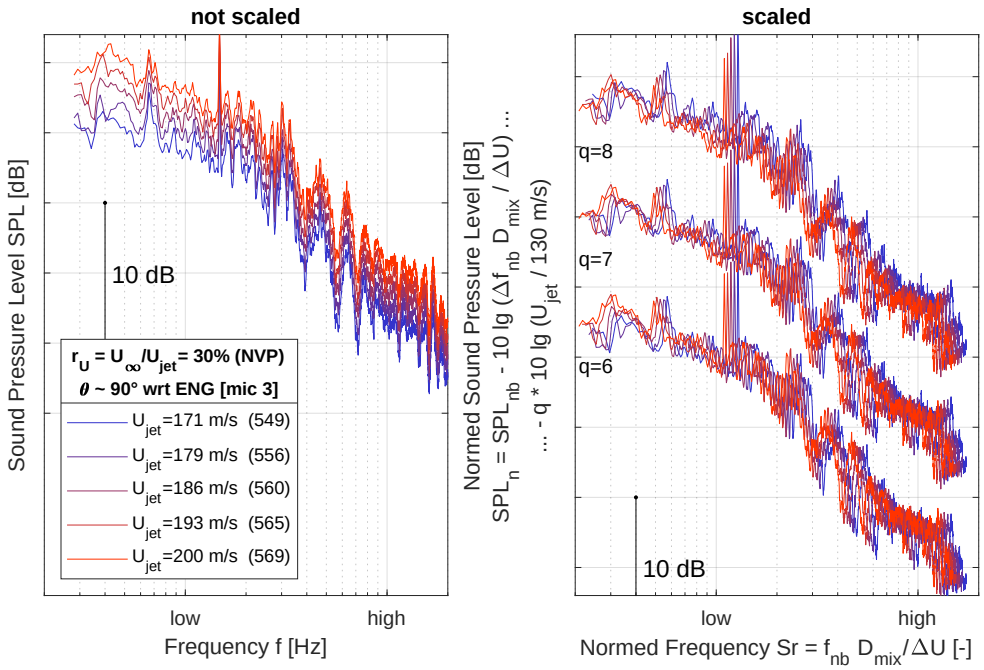

Figure 10: $I \propto U_{jet}^{q}$ velocity scaling for $r_U = 30\,\%$=const.

Jet and windtunnel speeds were calculated by using the following relationships:

$$U_{jet}\left(\Delta U, r_U\right) = \frac{1}{1 - r_U} \cdot \Delta U \tag{71}$$

$$U_{\infty}\left(\Delta U, r_U\right) = \frac{r_U}{1 - r_U} \cdot \Delta U \tag{72}$$

$$\text{Note, that: } \Sigma U\left(\Delta U, r_U\right) = \frac{1 + r_U}{1 - r_U} \cdot \Delta U \tag{73}$$

The scaled experimental data:

- scales well at $n = 2$, especially for high frequencies and slightly underscales at higher difference velocities,
- scales well at $n = 3$, especially for high and low frequencies.
- overscales at $n = 4$ for high frequencies and only slightly overscales for low frequencies.

Note, that the scaling coefficient $n = 3$ delivers reasonable scaling results with the experimental data. The corresponding velocity ratios r_U are very close or even within the critical velocity ratios derived in equations 44 and 47. This may tend to support a changing velocity scaling law hypothesis (see equation 48).

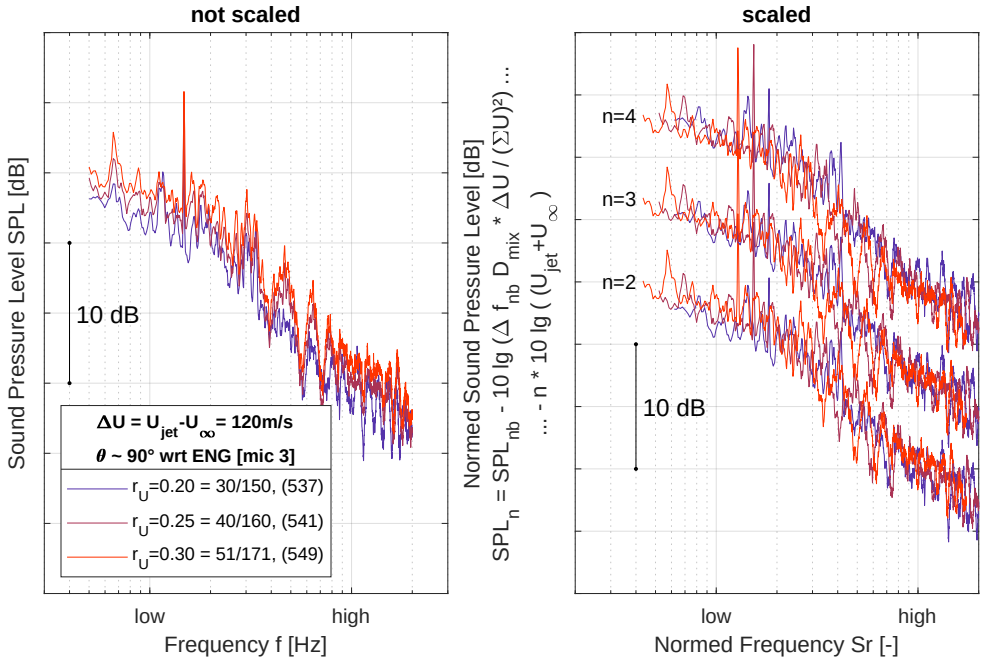

Figure 11: $I \propto U_c^n$ velocity scaling for $\Delta U = 120\,\mathrm{m/s} = \mathrm{const}$, $\overline{U} < \Delta U$

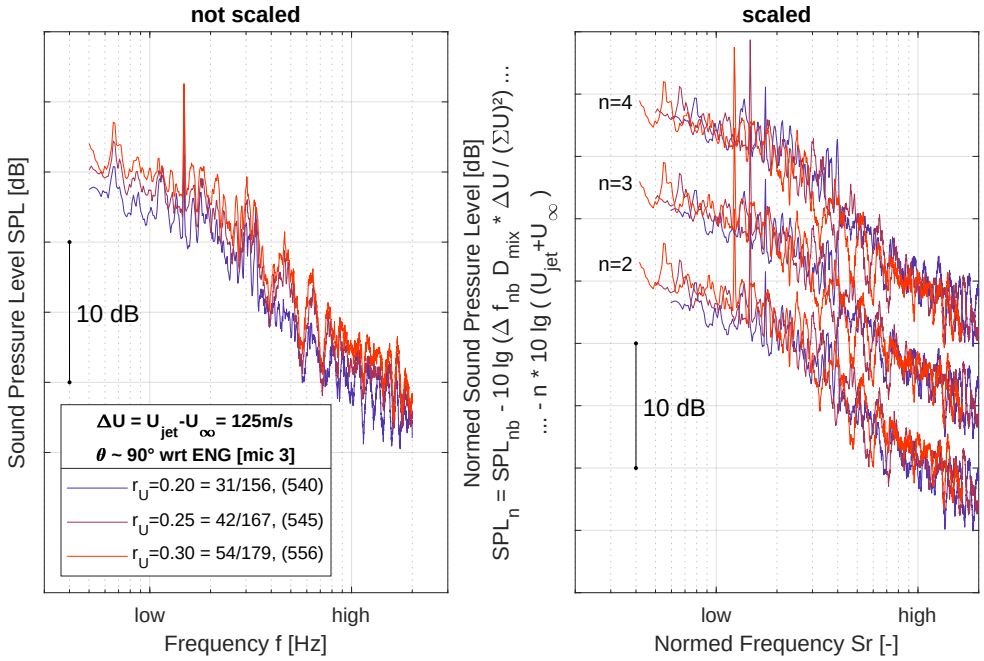

Figure 12: $I \propto U_c^n$ velocity scaling for $\Delta U = 125\,\mathrm{m/s} = \mathrm{const}$

III.C. The dependency on shear layer difference speed

Similar convection velocities are not easily created if the convection parameter $c(r_U)$ cannot be estimated correctly. However, it is easily possible to measure velocity profiles with the same mean velocity in the shear layer, here $\overline{U} = 125\,\mathrm{m/s}$, i.e. $\Sigma U = 250\,\mathrm{m/s}$. Those velocity profiles are supposed to scale with $I \propto\!\!\propto (\Delta U)^6$ for low velocity ratios.

$$I \propto \cdot (\Delta U)^6 \, (c(r_U))^2 \cancel{(\Sigma U)^2}^{const.} \tag{74}$$

$$Sr \propto \frac{f \cdot D_{mix} \cdot \Delta U}{c^2} \cdot \cancel{(\Sigma U)^{-2}}^{const.} \tag{75}$$

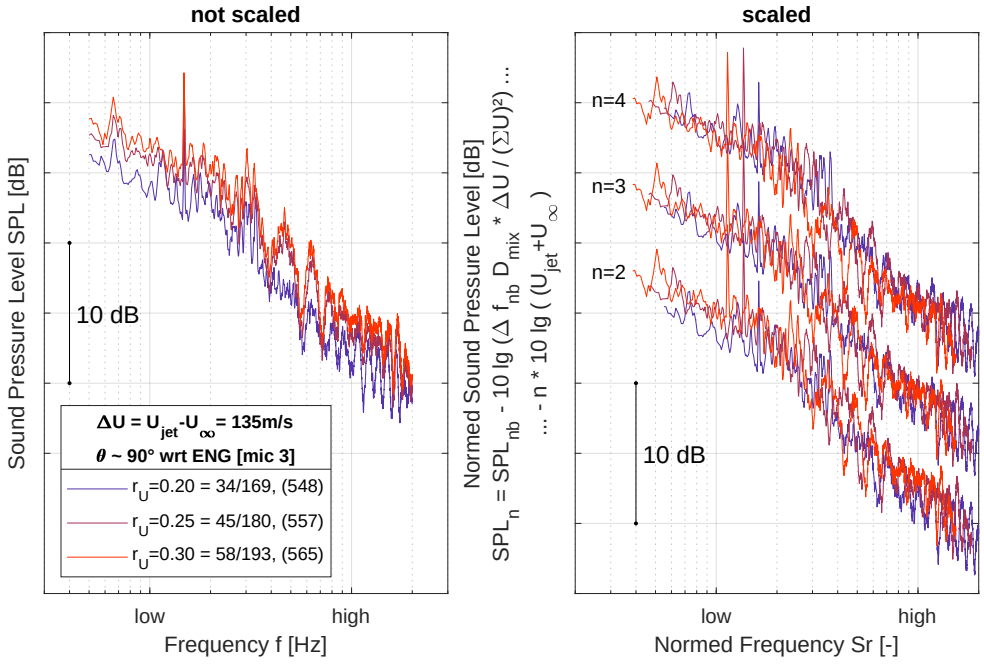

Figure 13: $I \propto U_c^n$ velocity scaling for $\Delta U = 135\,\mathrm{m/s} = \mathrm{const}$

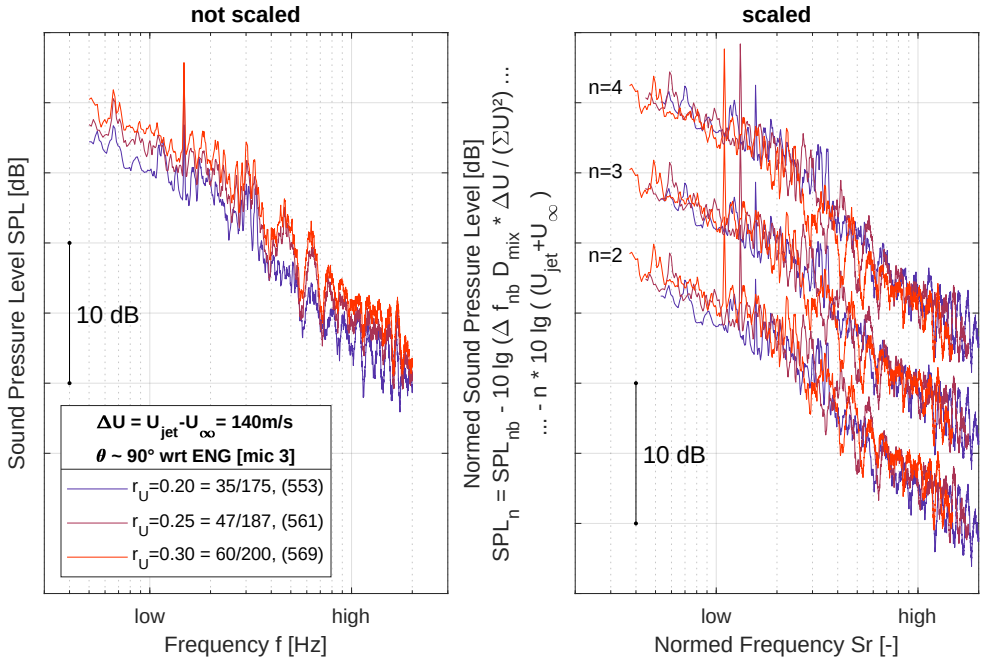

Figure 14: $I \propto U_c^n$ velocity scaling for $\Delta U = 140\,\mathrm{m/s} = \mathrm{const}$

Jet and windtunnel speeds are calculated by using the following relationships:

$$U_{jet}\left(\Sigma U, \Delta U\right) = \frac{\Sigma U + \Delta U}{2} \tag{76}$$

$$U_{\infty}\left(\Sigma U, \Delta U\right) = \frac{\Sigma U - \Delta U}{2} \tag{77}$$

$$\text{Note, that: } r\left(\Sigma U, \Delta U\right) = \frac{\Sigma U - \Delta U}{\Sigma U + \Delta U} \tag{78}$$

The unscaled spectra (figure 15) show a SPL difference of $\Delta SPL \approx 7\,\mathrm{dB}$, which is favorable for good velocity scaling. The normalized spectra tend to:

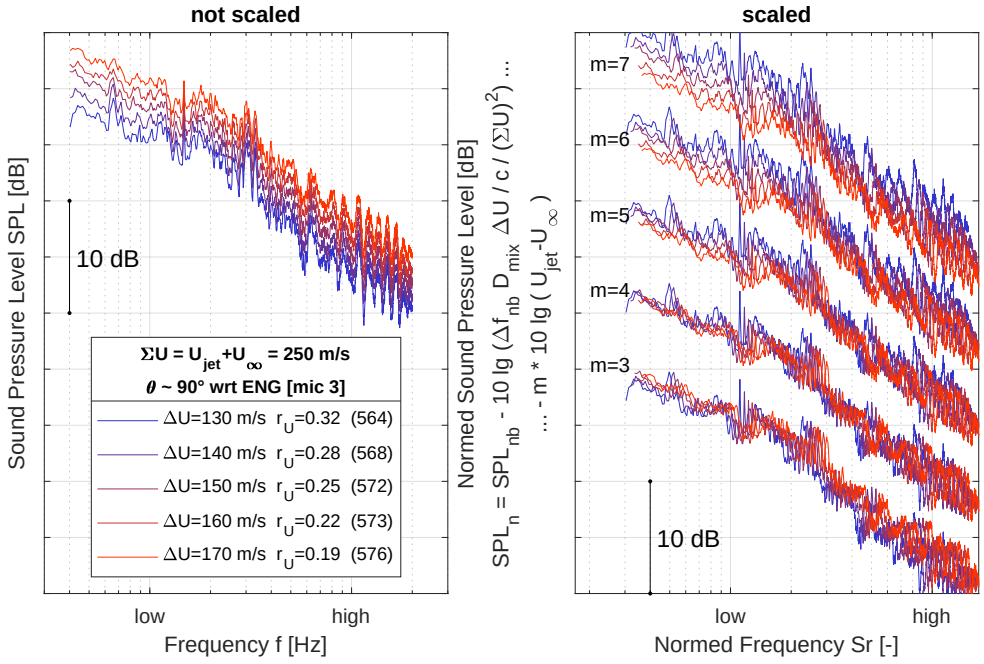

Figure 15: $I \propto (\Delta U)^m$ velocity scaling for $\Sigma U = 250\,\mathrm{m/s} = \text{const.}$

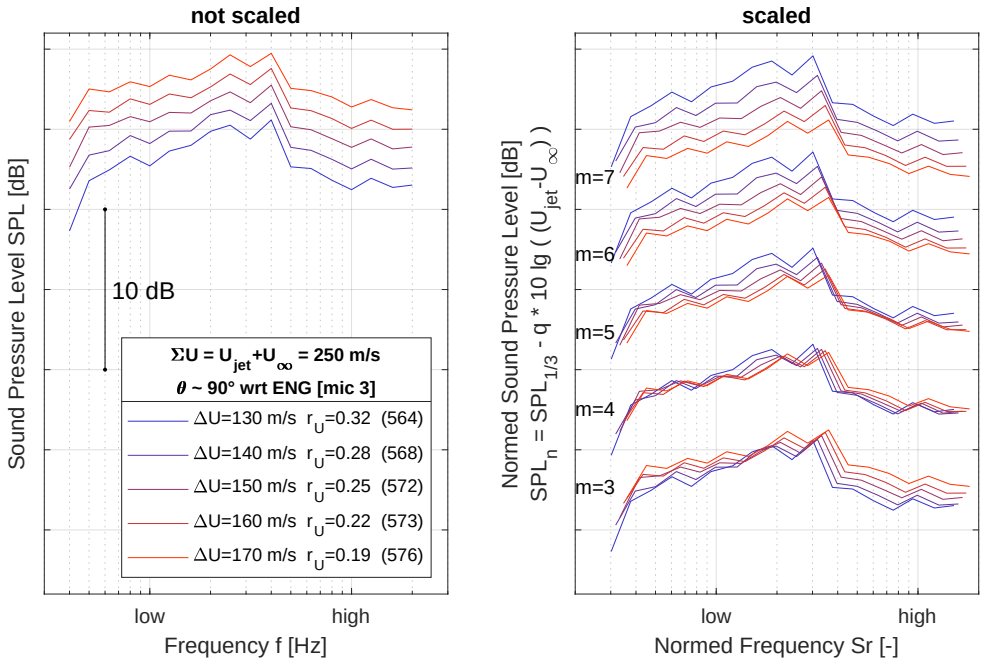

Figure 16: $I_{1/3} \propto (\Delta U)^m$ velocity scaling for $\Sigma U = 250\,\mathrm{m/s} = \text{const.}$

- underscale at $m = 3$,
- scale well at $m = 4$ for the low frequencies,
- scale well at $m = 5$, especially for high frequencies,
- overscale for $m = 6$, whereby merely high frequencies of low velocity ratio datapoints might still scale well,
- overscale for $m = 7$

With those experimental results, an experimental scaling exponent of $n = 4 \ldots 5$ appears to be reasonable. This is surprising, since scaling of presumably strong and intermediate normal velocity profiles would

favor a factor of $m = 5$ with a tendency to $m = 6$. Thus, this results supports the hypothesis of changing velocity scaling laws (equation 48) and tends to give indication that velocity profiles of velocity coefficients as low as $r_U \geq 0.3$ present weak NVP and tend to scale similarly to the hypothetically proposed near unity region derivation $m = 4$.

In order to challenge this, combined velocity scaling shall be tested out.

III.D. Combined Scaling for similar Strouhal number and high velocity ratios

First of all, high velocity ratios $r_U \approx 0.3$ shall be tested, whereby the Strouhal number is approximately constant. This test case shall be used for combined scaling (see equation 79), whereby a combined power 8 velocity scaling dimension $q = m + n = 8$ is assumed. The exponents m and n are chosen to represent

- the theoretical derivation $(m = 6, n = 2)$ which should theoretically apply for strong NVPs.
- the alternative theoretical derivation $(m = 4, n = 4)$, which might apply well for near unity NVPs.
- exponents in between $(m = 5, n = 3)$, which might be a relevant matching condition for intermediate NVPs.

$$I \propto \cdot (\Delta U)^m \, (\Sigma U)^n (c(r_U))^n \tag{79}$$

The velocity scaling results in figure 17 show how different rather weak NVP cause noise spectra which:

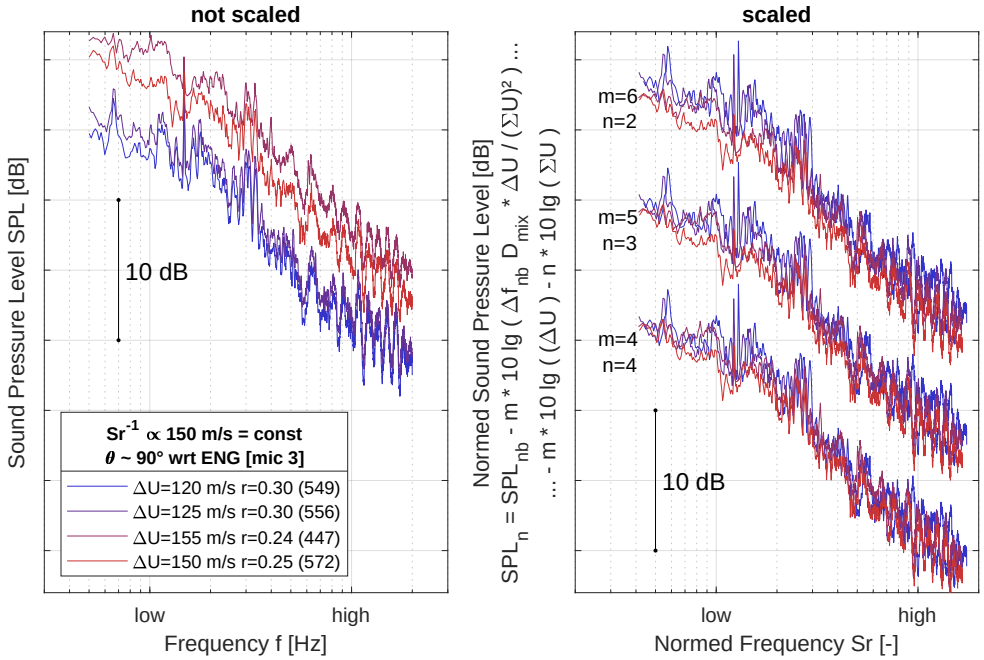

Figure 17: $I \propto (\Delta U)^n U_c^m$ velocity scaling for $Sr_c^{-1} \propto 150\,\mathrm{m/s} = \text{const}$.

- underscale for $[m = 6, n = 2]$, especially for the low frequency peak.
- slightly underscale at $[m = 5, n = 3]$.
- scale very well for $[m = 4, n = 4]$.

This result is another support for the changing velocity scaling exponent hypothesis.

III.E. Combined Scaling for constant jet speed

A very common test situation is the testing of different flight speeds, e.g. $U_\infty = 40\,\mathrm{m/s} \ldots 60\,\mathrm{m/s}$, for a fixed engine setting, thereby producing normal velocity profiles ($r_U < 1$). Note, that this is one of the few datasets, where a larger number of truely strong velocity profiles are scaled. The velocity scaling results in figure 18 show how different NVP cause noise spectra which:

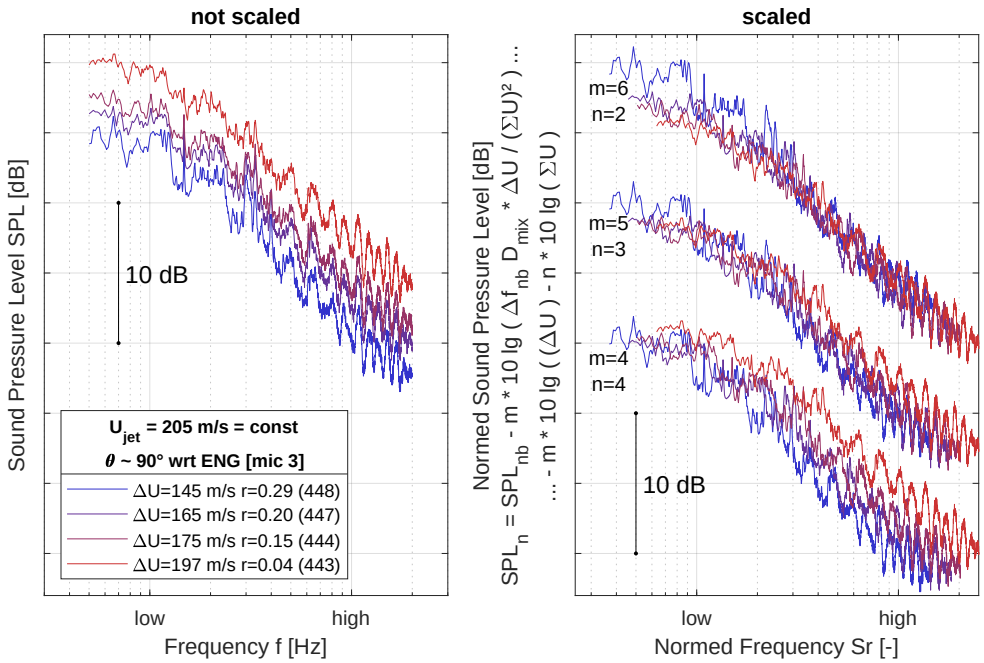

Figure 18: $I \propto (\Delta U)^n U_c^m$ velocity scaling for $U_{jet} = 205\,\mathrm{m/s} = \text{const}$.

- scale great for $[m = 6, n = 2]$, especially for the high frequencies. The highest velocity ratio $r_U = 0.29$ overscales in the low frequency region. This result is in agreement with the derivations for low velocity ratios!
- slightly underscale at $[m = 5, n = 3]$ for high frequencies. Note, that the low (peak) frequencies are in good agreement. This makes $[m = 5, n = 3]$ a good candidate for experimental results.
- underscale for $[m = 4, n = 4]$.

Note, that the scaling results show (see exponent m) as well, that the low frequency peaks of strong normal velocity profiles scale well with $I \propto (\Delta U)^{4...5}$ when varying flight speed. This could lead to a wrong interpretation where test rig noise is assumed as a dominant sources due to power 5 scaling (rather than power 8 scaling). In the following section shall be shown, why $I \propto (\Delta U)^5 \cdot U_{jet}^3$ is a great approximation for $I \propto \Delta U^6 {U_c}^2$ at constant jet speed.

IV. Approximation for velocity scaling of normal velocity profiles

Conventional velocity scaling is based on using a difference velocity approach $I \propto \Delta U^q$. The interesting question is how is this approximative scaling related to the $I \propto \Delta U^6 {U_c}^2$ (for $r_U \to 0$) derivation in this paper. As a side condition, the velocity profiles of the previous sections are used. This means that jet velocity is a constant whereas flight velocity varies.

IV.A. Derivation

Starting from the former derived relation (equation 80), the idea is to get a relation for Intensity I depending on difference speed ΔU alone, whereby the jet speed U_{jet} (i.e. a constant) is also allowed. Such a derivation leaves an approximation error which must be negligible. The decompositions for exponents $n = 4 \ldots 6$ are derived in equations 81 to 83 and the approximation error is shown for normal velocity profiles (yet valid for $r_U < 0.25$) see figure 19).

$$I \propto (\Delta U)^6 \left(U_{jet} + U_\infty\right)^2 \cancelto{\text{assume negligible}}{\left(c(r_U)\right)^2} \tag{80}$$

$$n = 6 : I \propto (\Delta U)^6 \, U_{jet}^2 \left(1 + r_U\right)^2 \tag{81}$$

$$n = 5 : I \propto (\Delta U)^5 \, U_{jet}^3 \left(1 - r_U\right) \left(1 + r_U\right)^2 \tag{82}$$

$$n = 4 : I \propto (\Delta U)^4 \underbrace{U_{jet}^4}_{\text{const}} \underbrace{\left(1 - r_U\right)^2 \left(1 + r_U\right)^2}_{\text{approx. error}} \tag{83}$$

$$\tag{84}$$

Note, how the approximation error for $n = 5$ looks similar to a Taylor series like polynomial of order 3, whereby the linear term r_U is compensated by the combination of the quadratic and cubic term $r_U^2 + r_U^3$ (see equation 85).

$$I \propto (\Delta U)^5 \cdot U_{jet}^3 \cdot \cancelto{\approx 1 \text{ for NVP}}{\left(1 + r_U - r_U^2 - r_U^3\right)} \tag{85}$$

Since jet noise scaling is typically characterized by slight overscaling of smaller jet velocities, small

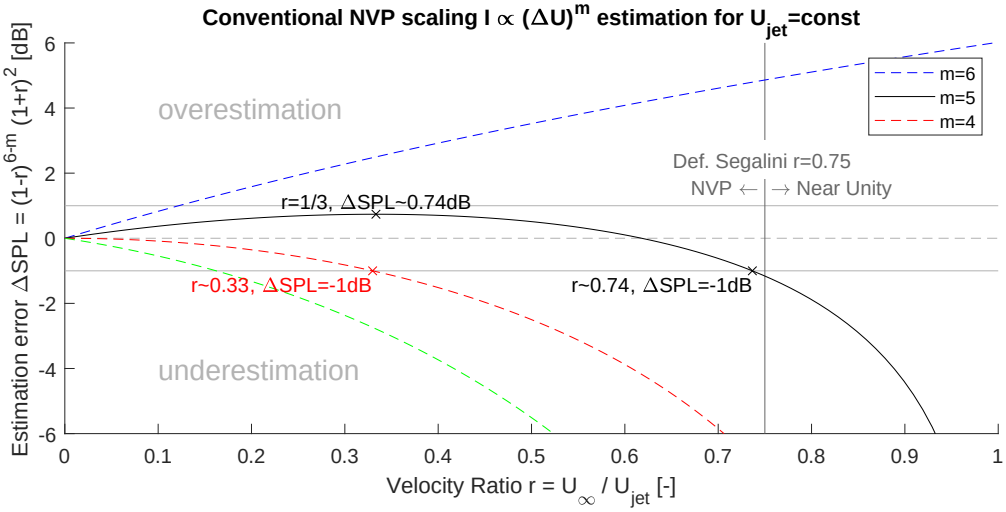

Figure 19: Estimation error of $I \propto \Delta U^m$ relation to $I \propto \Delta U^6 {U_c}^2$ at constant jet speed for various exponents m

approximation errors might come in handy to compensate the overscaling.

V. Summary: Jet scaling with coflow

This section shall explain how $I \propto (\Delta U)^m \cdot {U_c}^n$ velocity scaling can be summarized based on the previous derivations and experimental results. The visual summary is figure 20, which describes velocity scaling along the isocontours of constant velocity ratio (compare section III.A), difference speed (compare section III.B) and convection velocity (compare section III.B) as well as the derived velocity regions:

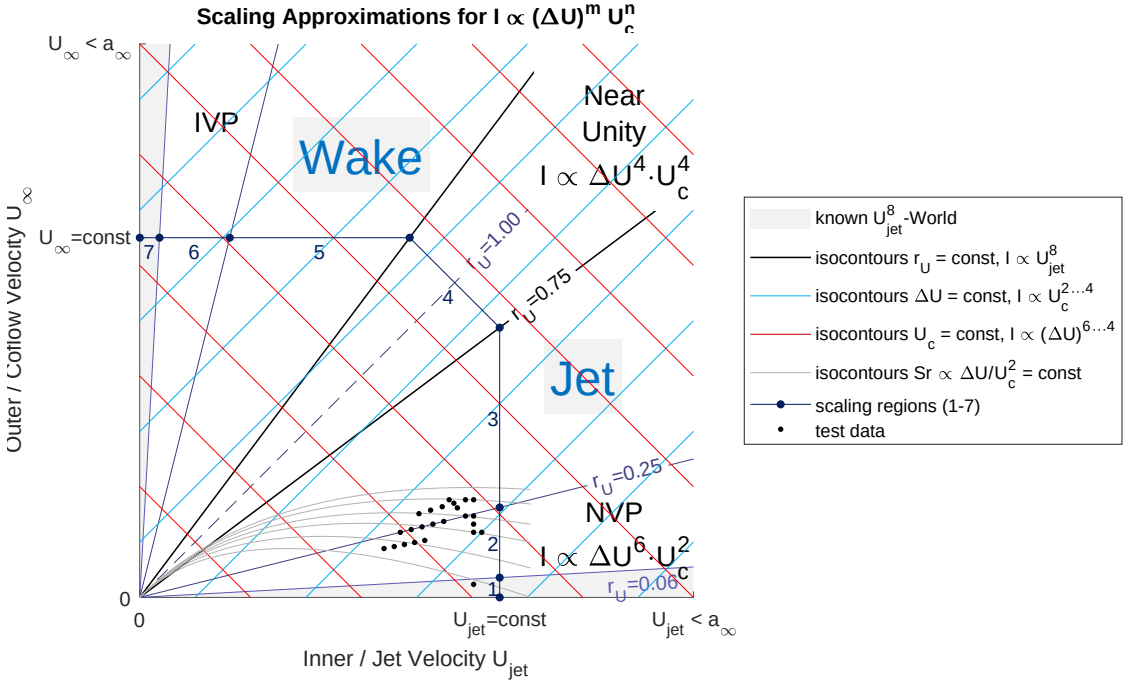

Figure 20: Velocity scaling approximations for $I \propto (\Delta U)^6 \cdot {U_c}^2$ derivation

1. Region of $I \propto U_{jet}^8$-Law: Very strong normal velocity profiles correspond to small velocity ratios of $r \leq 0.06$ and scale with the $I \propto U_{jet}^8$-law within an error margin of $\Delta SPL \leq 1\,\mathrm{dB}$. Note, that the $I \propto U_{jet}^8$-law scales with an error margin of $\Delta SPL = 2\,\mathrm{dB}$ until velocity ratios of $r_U \leq 0.10$.

2. Strong NVP Region: In the strong NVP-region, here defined with velocity ratio $0.06 < r_U < 0.25$, the difference velocity ΔU is greater than the shear layer convection velocity U_c. The velocity scaling law is $I \propto (\Delta U)^6 \cdot U_c^2$. The transition to the weak NVP-region has been approximated to occur in the range of velocity ratios $0.25 < r_U < 0.33$, whereby experimental data indicates that the transition occurs rather at the lower end $r_U \to 0.25$.

3. Weak NVP Region: The weak NVP-region can be defined for velocity ratios of $0.25 < r_U < 0.75$ and scales approximately with $I \propto (\Delta U)^5 \cdot U_c^3$ for lower velocity ratios around $r_U \approx 0.25$. The velocity region is defined by shear layer convenction speed being greater than the shear layer difference velocity. There is some indication in the experimental data, which hints that a transition to $I \propto (\Delta U)^4 \cdot U_c^4$ might occur for rather low velocity ratios r_U.

4. Near Unity Region: The Near Unity region is here defined by velocity ratios of $0.75 < r_U < 1.6$ (very weak NVPs $0.75 < r < 1$, unity $r = 1$ and very weak IVPs $1 < r_U < 1.6$) and scales with $I \propto (\Delta U)^4 \cdot U_c^4$. The velocity ratio limits have been defined corresponding to Segalini's[6] experimentally found near unity limits, where the velocity regions were identified by plotting isocontours of the maximum peak frequency as a function of outer to inner Reynolds number. Note the singularity for $r_U = 1$ where the (ideal) shear layer vanishes and ideally no sound is produced. Note, that the following IVP velocity regions are proposed in an inverted, but similar fashion to the NVP velocity regions.

5. Weak IVP Region: A weak IVP-region is is defined by the shear layer difference speed being smaller than the convection speed $|\Delta U| < U_c$.

6. Strong IVP Region: Strong inverted velocity profiles are defined by the shear layer difference speed being greater than the convection speed $|\Delta U| > U_c$.

7. Dead Wake Region: For very strong inverted velocity profiles, the jet flow assymptotically approximates zero, thus changing the function of the jet nozzle as a flow sources to dead wake behind a blunt (nozzle) body.

VI. Conclusion

The velocity scaling for noise of an cold jet in a co-flowing flight stream (isothermal shear layer) has been derived using a new approximation to account for the source volume, especially in the initial flow region. For the resulting velocity scaling law, a hypothesis has been formulated which states, that the scaling law exponents change depending on the velocity region:

- For small velocity ratios $r_U \to 0$ (strong NVPs), where difference velocity is greater than the convection velocity: Scaling with 6th power of the difference velocity and the convection velocity squared.
- For near-unity velocity ratios $r_U \to 1$, where the shear layer convection velocity is greater than the difference velocity: Scaling with 4th power of the difference velocity and the 4th power of the convection velocity.
- A transition of the scaling law approximately at velocity ratios $r_U \approx 0.25$, where difference velocity and convection velocity match: Scaling with the 5th power of the difference velocity and the third power of the convection velocity.

A windtunnel experiment has been conducted at the AWB test facility in Braunschweig, Northern Germany. The tested shear layer flows consist of strong, transitional and weak normal velocity profiles (NVP) with velocity ratios of $r_U = 0.15 \ldots 0.32$. The following conclusions where drawn based on theory and experiment:

- Without co-flow or for similar velocity profiles, the scaling equation reduces into Lighthill's widely known power 8 law. Thus, the derivation is consistent to conventional acoustic theory. By experimental means an exponent of $q = 7 \ldots 8$ could be confirmed. Slight scaling nonconformities are qualitatively comparable to the findings by other authors.
- Velocity profiles with the same difference velocity ΔU were especially compared for transitional and weak NVPs. Therefore, they scale with the convection speed to the power of 3 and 4 rather than with the convection speed squared.
- Velocity profiles with a similar mean flow speed $\bar{U}$ where examined for transitional and weak NVPs. They scale with the $4^{th} \ldots 5^{th}$ power of the difference velocity.
- This deviation from the scaling factors $[m = 6, n = 2]$ is a support to the hyposthesis of changing scaling coefficients depending on shear layer physics.
- For some test cases, the estimation of the correct convection speed is essential for velocity scaling. An approximation for the convection parameter c has been suggested. However, the approximation may need to be improved and tested by more experimental results.
- Based on the previously achieved result, a combined velocity scaling approach for $I \propto \Delta U^m \cdot {U_c}^n$ delivers good scaling for the exponent pairs $[m = 6, n = 2]$ as well as $[m = 5, n = 3]$ for strong and transitional NVPs, and $[m = 4, n = 4]$ for weak NVPs.
- The existing velocity profile types NVP, Near Unity and IVP can now be further devided into different velocity regions. The velocity scaling and approximate scaling for jet-like velocity profiles is presented in this paper. Any investigations for wake-like velocity profiles could not be tested and are candidates for future work.

Acknowledgments

The authors thank and acknowledge the support of DLR experts who helped out with their theoretical knowledge in their field, feedback and discussions, i.e. Jan Delfs on the derivation of general acoustical analogies and ideas for an experimental approach as well as Bernhard Eisfeld and Nan Hu on mixing layer theory. Furthermore, thanks to the entire test team at AWB for their precise and accurate work, patience and stamina during the hot summer testing days.

References

[1]Michalke, A. and Michel, U., "Prediction of jet noise in flight from static tests," *Journal of Sound and Vibration*, Vol. 67, No. 3, 1979, pp. 341–367.

[2]Lighthill, M. J., "On sound generated aerodynamically I. General theory," *Proceedings of the Royal Society of London. Series A. Mathematical and Physical Sciences*, Vol. 211, No. 1107, 1952, pp. 564–587.

[3]Fuchs, H. and Michel, U., "Experimental evidence of turbulent source coherence effecting jet noise," *4th Aeroacoustics Conference*, Aeroacoustics Conferences, American Institute of Aeronautics and Astronautics, 1977.

[4]Eisfeld, B., "Reynolds Stress Anisotropy in Self-Preserving Turbulent Shear Flows," .

[5]Gaeta, R. and Ahuja, K., "Subtle Differences in Jet Noise Scaling with Narrow Band Spectra Compared to 1/3-Octave Band," *9th AIAA/CEAS Aeroacoustics Conference and Exhibit*, Aeroacoustics Conferences, American Institute of Aeronautics and Astronautics, 2003.

[6]Segalini, A., *Experimental analysis of coaxial jets: instability, flow and mixing characterization*, Ph.D. thesis, Università di Bologna, Bologna and Italy, 01.01.2010.